5.6. ELECTRON-MOLECULAR ION COLLISIONS: EXPERIMENTS AND THEORY

M. Larsson, S. Rosén, A. Al-Khalili, A. Le Padellec, L. Vikor

Department of Physics, Stockholm University, Frescativ. 24, S-104 05 Stockholm, Sweden

Å. Larson, J. Semaniak, I.F. Schneider, C. Strömholm

Department of Physics, KTH, S-100 44 Stockholm, S-100 44 Stockholm, Sweden

S. Datz

Oak Ridge National Laboratory, Oak Ridge, TN, USA

W.J. van der Zande, R. Peverall

FOM Institute for Atomic and Molecular Physics, Amsterdam, The Netherlands

J.R. Peterson

Molecular Physics Laboratory, SRI International, Menlo Park, USA

G.H. Dunn, N. Djuric

JILA, University of Colorado, Boulder, Co, USA

A. Suzor-Weiner

Laboratoire Photophysique Moleculaire, Université Paris-Sud, Paris, France

Ann Orel

UC Davies, California, USA

H. Danared, M. af Ugglas

Manne Siegbahn Laboratory

1. Introduction

The experimental work at CRYRING aiming at an understanding of electron-molecular ion interactions has made great progress during 1997. It has been directed along several different lines: dissociative recombination of diatomic molecular ions, including both absolute cross sections, final states branching ratios and angular distributions; recombination cross sections and branching ratios of polyatomic molecular ions of astrophysical interest; non-crossing recombination cross sections; dissociative excitation of diatomic and polyatomic molecular ions; dissociative ionization; and theoretical work related to rotational effects and final state distributions.

2. Dissociative recombination; experimental

2.1. Cross sections for diatomic ions

Carbon monoxide (CO) is the second most abundant molecule in the universe after molecular hydrogen, and it is present in a wide variety of astrophysical environments, from the hot diffuse clouds to the denser and colder molecular clouds such as the dark clouds and the giant molecular complexes associated with H_{II} regions. Since H_2 is not directly observable, CO is used as a tracer to map the molecular hydrogen in the Milky Way as well as in other galaxies, a procedure performed basically by means of millimeter radio astronomy techniques. Observations also show CO in other astrophysical objects such as circumstellar envelopes, bipolar flows associated with birthplaces of stars, and planetary or cometary atmospheres. In all these media, its abun-

dance with respect to H_2 is determined mainly by the photodissociation rate in the ambient UV radiation field. On the other hand, singly charged carbon monoxide has been detected so far in only a few astrophysical environments, for instance toward the interfaces between molecular clouds and H_{II} regions around massive O stars. In addition, its abundance compared with other ions was determined to be rather small, which can be understood in the framework of fast conversion of CO^+ into HCO^+ by reaction with H_2. Hence, CO^+ is usually of significant abundance only in the hot layers of photon-dominated regions (called PDR's), where a significant fraction of hydrogen is present in atomic form.

Figure 1 presents the DR rates of Co^+ as a function of the center of mass energy [2]. For a given center of mass collision energy, one can run the electrons either slower (negative electron energy jumps) or faster (positive electron energy jumps) than the ions. The electron beam at zero collision energy had an energy of only 64.7 eV. Experiments with negative jumps were only possible over a limited range. The center-of-mass collision energies have been corrected for the space charge effect. The error bars in the figure are purely statistical at the one sigma level and thus represent the *relative* uncertainty, or uncertainty in the *shape* of the curve. In addition to the statistical relative uncertainties, there are also absolute systematic uncertainties which must be considered. The systematic uncertainty in ion current measurement is estimated to be about 3% (a new pickup coil has been installed since previous measurements), the circumference is uncertain to less than 1%, the electron current is measured to 2% accuracy and the current distribution is uncertain to no more than 7%, and the uncertainty in the electron cooler length is estimated to be on the order of 10%. Combining these sources of error yields a total systematic uncertainty of about 13% estimated to be at a level equivalent to one sigma. Thus, the whole curve in fig. 1 could be shifted up or down by 13% within the uncertainty.

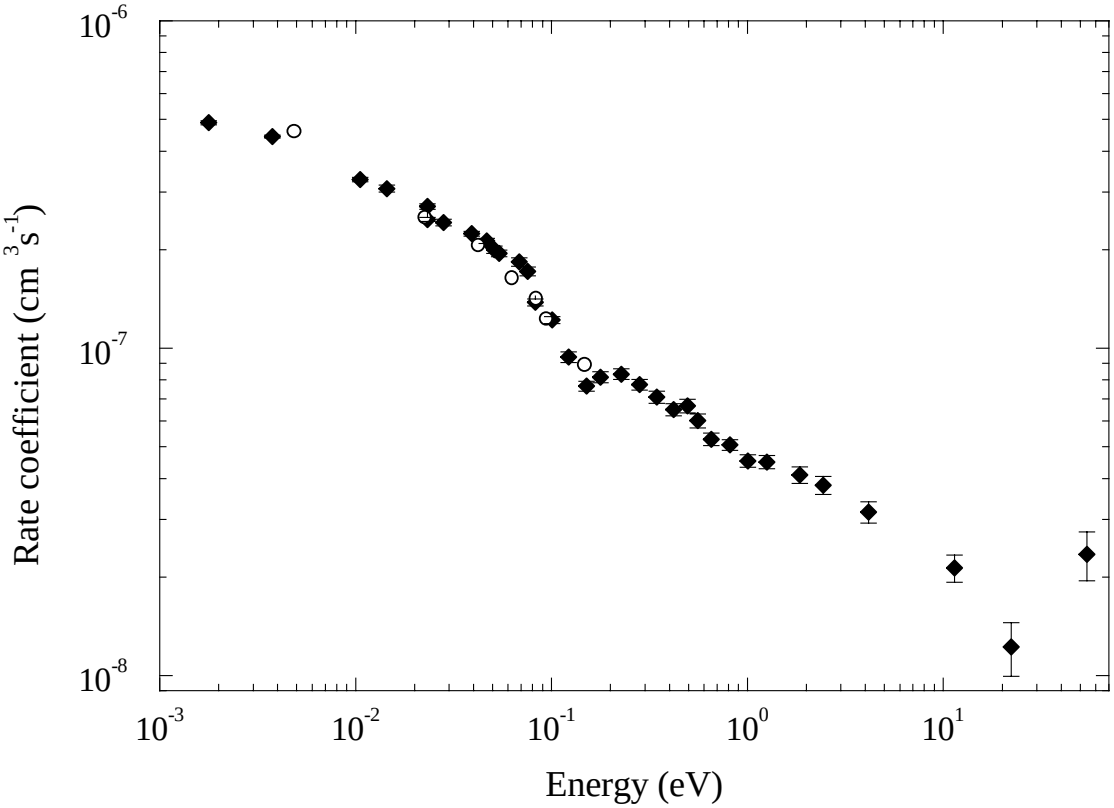

Figure 1. Absolute dissociative recombination rate coefficient, measured from 1 meV to 54 eV relative energy between electrons and ions. Filled dimonds shows data taken for $V_e > V_{ions}$ and open circle shows data taken for $V_e < V_{ions}$. The maximum observed rate defined our zero detuning energy.

A molecule like N_2^+ is clearly more difficult since it does not vibrationally relax in the ring (lack of dipole moment). For this reason, we used the JIMIS

hollow cathode source to precool the ions prior to extraction from the source. The vibrational temperature of the stored ions were then estimated by means of the imaging technique described in section 2. This means that the cross section is given for a known vibrational distribution. The thermal rate coefficient for N_2^+ (46% v=0, 27% v=1) versus electron temperature T_e is $1.75(\pm 0.09)\times 10^{-7}$ $(T_e/300)^{0.30}$ $cm^3 s^{-1}$ [2].

Molecules such as N_2^+ and O_2^+ are important constituents of the Earth's ionosphere. Recently, the generation of the atomic oxygen green line by dissociative recombination has been the focus of much interest [3,4]. We have recently investigated the dissociative recombination properties of O_2^+, both in terms of recombination cross sections and final state branching ratios. The results are so far only preliminary. The JIMIS hollow cathode source was used to vibrationally cool O_2^+ before extraction.

During the fall of 1997, the new 1 meV-tranverse-temperature electron beam was taken into operation in CRYRING. HeH^+ was chosen for a first experiment, because this system is an example of a non-crossing dissociative recombination molecule, and its recombination cross section is known to contain many resonances. Using the new electron beam we found a double-peak structure at 30 and 60 meV, and a Fano-like resonance at 15 meV [5]. The measured rate coefficient $\langle v\sigma \rangle$ is shown in figure 2.

2.2. Diatomic final state branching ratios

The asymptotic properties of dissociative recombination of diatomic ions are reflected in the amount of kinetic energy released in the process and the angular distribution of the products. These quantities can be measured by two-dimensional imaging of the DR products on a position-sensitive detector consisting of one or several microchannel plates (MCPs) linked to a phosphor screen and a charged-coupled-device (CCD) camera. If the difference in arrival time is measured, a complete three-dimensional image of the dissociation event is obtained.

The technique has been used to obtain final-state distributions in CO^+ [1], N_2^+ [2] and O_2^+. The results for N_2^+ has recently been published [2]. We report here on the results for CO^+.

For zero-energy collisions there are four energetically allowed limits, $O(^3P) + C(^3P)$, $O(^3P) + C(^1D)$, $O(^1D) + C(^3P)$, and $O(^3P) + C(^1S)$. For two of the higher collision energies, at 0.4 eV and 1.0 eV, for which spectra have been measured, there is an additional channel available, leading to the limit $O(^1D) + C(^1D)$ (endothermic at 0 eV collision energy, with an enthalpy change $\Delta H = +0.3$ eV). And for the collision energy of 1.5 eV there is a further limit available resulting in $O(^1S) + C(^3P)$ ($\Delta H = +1.25$ eV).

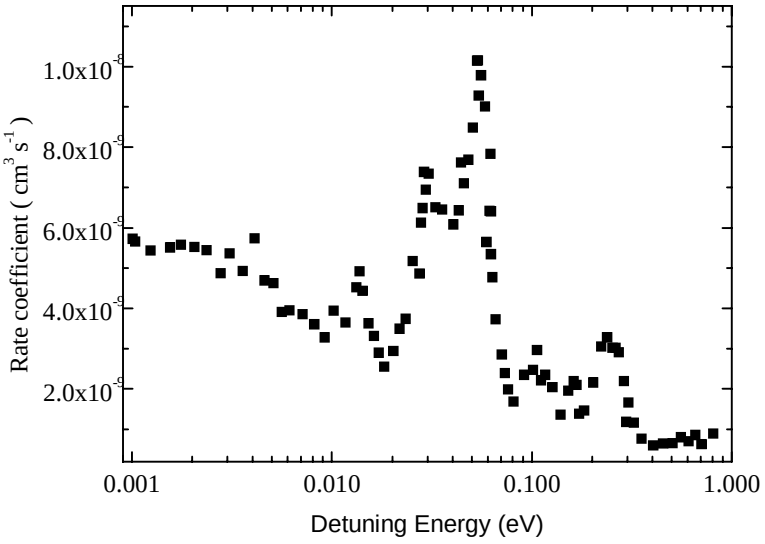

Figure 2. The rate coefficient for dissociative recombination of $^3HeH^+$ obtained with a transverse electron temperature of 1 meV.

The distribution of distances measured at 0 eV collisions is shown in fig. 3. Clearly, it can be seen that at this energy dissociative recombination mostly results in ground state atomic fragments ($O(^3P) + C(^3P)$): more than three quarters of all DR events lead to this limit (76%). The least exothermic limit ($O(^3P) + -c(^1S)$) is not observed. The other two dissociation limits, $O(^1P) + C(^1D)$ and $O(^1D) + C(^1D)$, have yields of 15% and 9%, respectively. The error in the fit to the 0 eV spectra is estimated to be ±5% of the branching ratios. We note that the distribution spectrum excludes the presence of vibrationally excited CO^+.

2.3. Polyatomic branching ratios

A polyatomic molecular ion ABC^+ may have different decay channels:

$$ABC^+ + e^- \rightarrow \begin{cases} A + B + C & (a) \\ AB + C & (b) \\ A + BC & (c) \end{cases}$$

In many applications, not least interstellar chemistry, it is important to know the DR branching ratios, that is (*a*), (*b*) and (*c*). This is a very difficult experimental problem, which has only been addressed in a few cases. An ion storage ring offers particular advantages for measuring branching ratios due to the high luminosity obtained with a circulating ion beam, and the high energy at which ions are stored.

Using a grid technique combined with an energy dispersive surface detector, the breakup pattern in dissociative recombination of CH_2^+ [6] and CH_5^+ [7] was measured. Formation of molecules in the interstellar molecular clouds is usually conceived of as consisting of dissociative recombination as the final step. This makes it important to determine the recombination branching ratios. CH_2^+ and CH_5^+ are

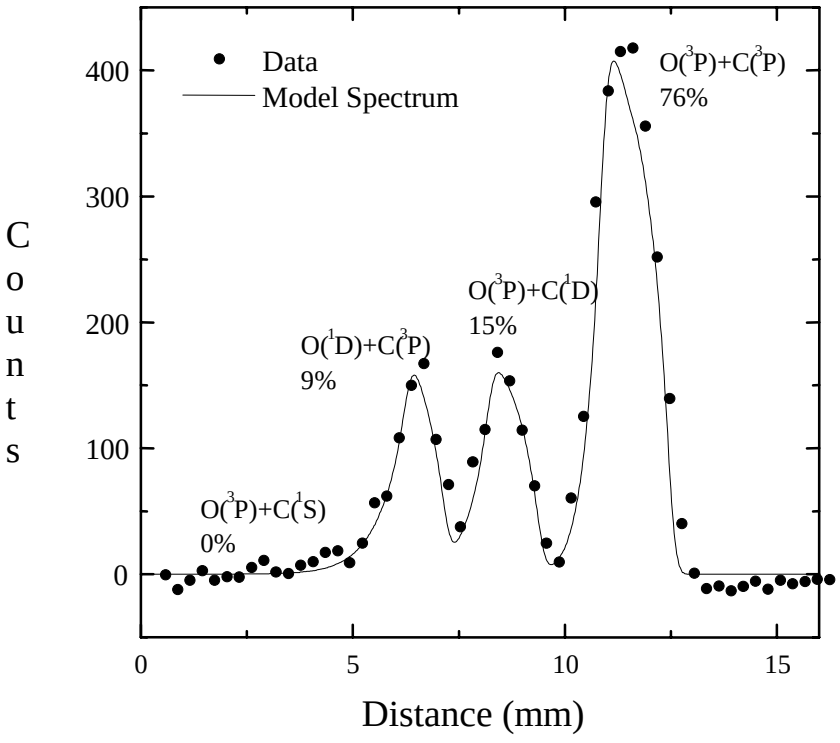

Figure 3. Distance spectrum for branching fraction determination in dissociative recombination of CO^+. (•) shows data taken at 0 eV electron energy; the full drawn line shows a fit with correction for timing cut off and detector efficiency.

both important interstellar molecular ions.

We found that CH_4 is formed in only 5% of the cases when CH_5^+ recombines with an electron. This is a much smaller branching fraction than what has been commonly believed.

CH_2^+ was found to follow mainly a three-body breakup, forming C+H+H. This is line with the general trend that dissociative recombination of polyatomic ions leads to significantly more fragmentation than earlier believed.

2.4. Dissociative excitation

If the electron has sufficient energy to excite a molecular ion into a repulsive electronic state, also charged fragments are formed. This process is labelled dissociative excitation. It has received less attention than dissociative recombination, but it plays an important role in the edge plasma of experimental fusion reactors. The process can be studied in CRYRING, and in several of the papers discussed in this Annual Report, we also publish results from dissociative excitation [1,2,6,7].

3. Theoretical calculations

The theoretical work has been directed along four lines: (i) what is the effect of rotational excitation on dissociative recombination; (ii) what is the final state distribution in the recombination of HeH^+; (iii) what is the mechanism causing dissociative recombination of H_3^+; and (iv) how is it possible that recombination of OH^+ at certain electron energies leads to an extremely small release of kinetic energy?

The multichannel quantum defect theory was used in a case study of HD^+ [8]. Electronic, vibrational and rotational interactions were included simultaneously. The effect of including the rotational interaction was studied by calculating the HD^+ dissociative recombination cross section for electron energies in the range 1 meV – 13 eV. The cross section measured in CRYRING was well reproduced in shape and size below 0.3 eV when the theoretical results were averaged over a 300 K Boltzmann distribution.

In a further study [9] it was found that rotational effects play a role mainly for the indirect process through bound Rydberg states, and for light molecules.

HeH^+ recombines effectively both at low electron energies, and at electron energies above 10 eV. The high energy recombination has been studied theoretically in order to understand the final state distributions. The results are so far preliminary [10].

Dissociative recombination of H_3^+ remains an enigma. The multichannel quantum defect theory has been applied. A direct process leading to recombination to the H_3 ground state seems possible to exclude.

Dissociative recombination of OH^+ was studied in CRYRING by means of the particle imaging technique. When the electron energy exceeded 1.64 eV, the very small kinetic energy release of 120 meV was measured. This is due to recombination leading to the formation of ground state oxygen and H(n=2). Most likely, this limit is reached by a redistribution of dissociating flux after electron capture into the $2\,^2\Pi$ state of OH [12]

4. Imaging detector

A microchannel plate/CCD-camera particle detector has been developed that utilizes gold strips deposited upon the surface of an MCP to provide particle arrival time information [13]. The uncertainty in the timing is about 500 ps.

The front end of the high-speed imaging consists of a set of three microchannel plates (MCPs) and a phosphor screen. The rear surface of the last MCP has 21 gold strips on it to record timing information. The MCPs are 25 mm in diameter. The MCPs provide a total gain of 10^8.

The imaging detector was used in [1,2,12], and a detector of similar type was used in [3].

5. Review

The field of dissociative recombination in ion storage rings has been reviewed [14]. A more popular account of the subject is given in [15].

6. References

[1] S. Rosén, R. Peverall, M. Larsson, A. Le Padellec, J. Semaniak, Å. Larson, C. Strömholm, W.J. van der Zande, H. Danared, and G.H. Dunn, Phys. Rev. **A57** (in press).

[2] J.R. Peterson, A. Le Padellec, H. Danared, G.H. Dunn, M. Larsson, Å. Larson, R. Peverall, C. Strömholm, S. Rosén, M. af Ugglas, and W.J. van der Zande, J. Chem. Phys. **108** (1998) 1978.

[3] D. Kella, L. Vejby-Christensen, P.J. Johnson, H.B. Pedersen, and L.H. Andersen, Science **276** (1997) 1530.

[4] S.L. Guberman, Science **278** (1997) 1276.

[5] A. Al-Khalili, H. Danared, M.Larsson, A. Le Padellec, R. Peverall, S. Rosén, J. Semaniak, M. af Ugglas, L. Vikor, and W.J. van der Zande, Hyperfine Interactions (in press).

[6] J. Semaniak, Å. Larson, A. Le Padellec, C. Strömholm, M. Larsson, S. Rosén, R. Peverall, H. Danared, N. Djuric, G.H. Dunn, and S. Datz, Astrophys. J. **498**, (in press)

[7] Å. Larsson, A. Le Padellec, J. Semaniak, C. Strömholm, M. Larsson, R. Peverall, H. Danared, N. Djuric, G.H. Dunn, and S. Datz, Astrophys. J. (in press)

[8] I.F.Schneider, C. Strömholm, L. Carata, X. Urbain, M. Larsson, A. Suzor-Weiner, J. Phys**. B30** (1997) 2687.

[9] B. Valcu, I.F. Schneider, M. Raoult, C. Strömholm, M. Larsson, and A: Suzor-Weiner, Europ. Phys. Rev. D (in press).

[10] Å. Larson and A. Orel, (in preparation).

[11] I.F. Schneider and A. Suzor-Weiner, (in preparation).

[12] C. Strömholm, H. Danared, Å. Larson, M. Larsson, C. Marian, S. Rosén, B. Schimmelpfennig, I.F. Schneider, J. Semaniak, A. Suzor-Weiner, U. Wahlgren and W.J. van der Zande, J. Phys. **B30** (1997) 4919.

[13] S. Rosén, R. Peverall, J. ter Horst, G. Sundström, J. Semaniak, O. Sundqvist, M. Larsson, M. deWilde, and W.J. van der Zande, Hyperfine Interactions (submitted).

[14] M. Larsson, Annu. Rev. Phys. Chem. **48** (1997) 151.

[15] M. Larsson, Kemisk Tidskrift no **6** (1997) 22.